Mon. Not. R. Astron. Soc. **000**, 000–000 (2007) Printed 4 November 2007 (MN LATEX style file v2.2)

Direct Observational Test Rules Out Small Mg II Absorbers

Andrew Pontzen[1⋆], Paul Hewett[1], Robert Carswell[1], Vivienne Wild[2]
[1] *Institute of Astronomy, Madingley Road, Cambridge CB3 0HA, UK*
[2] *Max-Planck-Institut für Astrophysik, 85748 Garching, Germany*

Accepted 2007 August 5. Received 2007 June 26.

ABSTRACT

Recent observations suggest the incidence of strong intervening Mg II absorption systems along the line-of-sight to gamma ray burst (GRB) afterglows is significantly higher than expected from analogous quasar sightlines. One possible explanation is a geometric effect, arising because Mg II absorbers only partially cover the quasar continuum regions, in which case Mg II absorbers must be considerably smaller than previous estimates. We investigate the production of abnormal absorption profiles by partial coverage and conclude that the lack of any known anomalous profiles in observed systems, whilst constraining, cannot on its own rule out patchy Mg II absorbers.

In a separate test, we look for differences in the distribution function of Mg II equivalent widths over quasar continuum regions and C III] emission lines. We show that these anomalies should be observable in any scenario where Mg II absorbers are very small, but they are not present in the data. We conclude that models invoking small Mg II cloudlets to explain the excess of absorbers seen towards GRBs are ruled out.

Key words: quasars: absorption lines

1 INTRODUCTION

The recent claim that strong Mg II absorption along the sightlines to gamma ray bursts (GRBs) is significantly more likely than along the sightlines to quasars (Prochter et al. 2006, hereafter P06) is puzzling. Subsequent results suggest that Mg II absorbers are unique in exhibiting this trend, C IV absorbers displaying population statistics independent of the nature of the background source (Tejos et al. 2007; Sudilovsky et al. 2007). One possibility is that some of the Mg II absorbers seen towards GRBs are intrinsic, although the high velocity separation between GRB and absorber coupled with the low velocity dispersion in the observed Mg II components prove a challenge to theoretical models. Therefore, it remains of interest to investigate possible explanations for the effect in terms of intervening absorbers.

This letter will focus on the model proposed by Frank et al. (2006, hereafter F06), which suggests geometric effects are responsible for the discrepancy. In this picture, the Mg II absorbers are somewhat smaller than the beam size of the quasar continuum region, whereas GRB beam sizes are smaller still. This would evidently lead to a difference in the observed distribution of absorber properties.

However, such small absorber sizes do not fit well with the established observational picture. Information on absorber sizes comes from studies of galaxies near quasar absorber sightlines, and from comparing absorber and galaxy number densities. These give typical radii ∼40 kpc for Mg II complexes, which may contain several velocity components, for a rest equivalent width limit of 0.3 Å (Steidel 1993; Zibetti et al. 2007). For lower equivalent width limits the inferred sizes are larger (Churchill et al. 1999), and projected Mg II absorber-galaxy correlation functions show a significant excess out to over 1 Mpc (e.g. Bouché et al. 2004). For individual velocity components of low ionization species, sizes are less than ∼300–400 pc (Rauch et al. 2002).

On the other hand, quasar continuum regions are generally considered to be orders of magnitude smaller. Important for the investigation presented here is the significant difference in the physical size of the ultraviolet continuum emitting region and the broad emission line region in luminous quasars. Constraints of the physical size of the broad line and continuum regions are provided by reverberation studies (e.g. Kaspi et al. 2005, 2007) and gravitational lensing studies (Lewis et al. 1998). Recently the latter method was used by Wayth et al. (2005), giving values of 0.02 pc for the continuum region, with a broad-line region > 3 times larger (possibly considerably larger than this lower limit).

A comprehensive analysis of possible routes to solving the GRB discrepancy has recently been presented by Porciani et al. (2007), wherein it is suggested that the model in F06 has severe weaknesses. These relate to the neglect of multiple clouds in the F06 model, and the difficulty in producing doublet ratios which are consistent with observations. Whilst Porciani et al. (2007) propose strong objections to the model, they do not rule it out. Furthermore, the

⋆ Email: apontzen@ast.cam.ac.uk

idea appears to have been gaining popularity and has been used to interpret recent observations (Hao et al. 2007).

In this letter, we provide direct observational evidence against the F06 model. First, we briefly discuss whether patchy absorbers can be ruled out on the basis of their absorption profiles and line ratios alone (Section 2), and conclude that this is not always the case. We then use the differing size of the quasar continuum and C III] emission region to provide a definitive test for the F06 model (Section 3). We provide a summary in Section 4.

2 PROFILES OF SINGLE VELOCITY COMPONENT PARTIAL ABSORBERS

Suppose quasars emit light with a hard-edged circular beam, radius R_e. Then a circular, single component Mg II absorber can be parametrized by its central column density ($N_{\rm MgII}$), velocity width (v) and its radius as a fraction of the beam radius (R_0/R_e). In practice the 'beam width' is an angular line-of-sight effect and will scale accordingly as $R_0 = \theta D_A(z)$ where z is the redshift of the absorber and D_A is the angular diameter distance. However, this geometric effect will be neglected as $D_A(z_{\rm abs}) \simeq D_A(z_{\rm em})$. We set $R_e = 1$ without loss of generality.

For $R_0 < 1$, providing that spectra of adequate S/N and velocity resolution are obtained, saturated profiles with a systematic offset above the zero-flux level (resulting from light 'leaking' around the edges) will be seen. However, it is not realistic to model absorbers with a hard edge; there must be a region around their edges where the column density drops. In the absence of any favoured theoretical or empirical model, we write:

$$N_{\rm MgII}(R) = \begin{cases} N_0 & R < R_0 \\ N_0 \left(\frac{R}{R_0}\right)^{-n} & R > R_0 \end{cases} . \quad (1)$$

During the drafting of this paper, a revised version of P06 independently proposed a similar model, using a three dimensional distribution:

$$\rho(r) = \begin{cases} \rho_0 & r < r_0 \\ \rho_0 \left(\frac{r}{r_0}\right)^{-k} & r > r_0 \end{cases} . \quad (2)$$

This latter model is less convenient for our purposes of computing high resolution profiles, something which P06 did not attempt. However, one may roughly relate the two distributions simply by integrating the second to yield $n = k - 1$ outside the core radius.

The resulting observed profile is calculated numerically as:

$$F(\lambda) \propto \int_0^1 2\pi R e^{-\tau_\lambda(N_{\rm MgII}(R), v)} {\rm d}R \quad (3)$$

where $\tau_\lambda(N, v)$ is a standard Voigt optical depth profile for Mg II λ2796, and $F(\lambda)$ is the observed flux. We separately calculate the somewhat weaker profile Mg II λ2803 so that we can fit for both components simultaneously. We take $v = 5$ kms^{-1}, which is the mean broadening for individual Mg II clouds (Churchill 1997).

The model spectra are realized at high resolution ($\delta\lambda = 0.01$Å in the absorber restframe). Gaussian random noise is added with S/N=100, to approximate the best available echelle spectra. We then fit a Voigt profile to the two components, assuming the correct ratio of oscillator strengths. The resulting reduced χ^2, measured over the region where the departure from continuum level is significant at the 1σ level, gives an indication of how well the partial absorber can fool one into believing the feature is due to a full coverage absorber, including the effect of the doublet ratio.

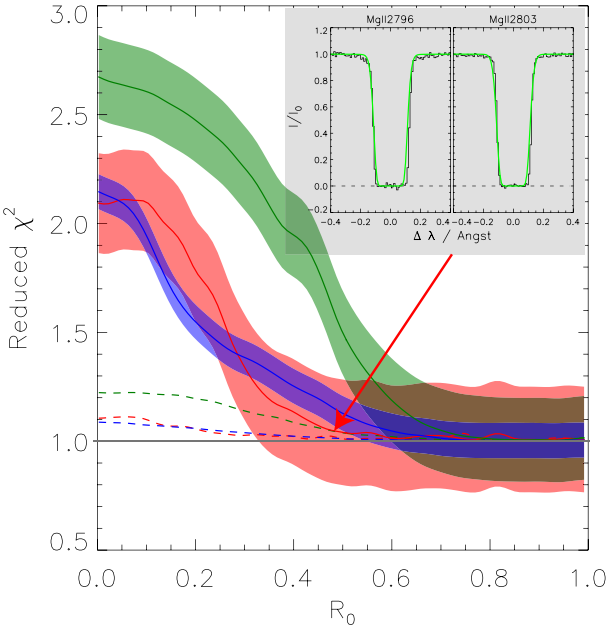

Figure 1. The reduced χ^2 of the best fit pure Voigt profile to a partial absorber with a core radius R_0 ($R_e = 1$), outside of which the column density decays as R^{-1} (dashed lines) and R^{-2} (solid lines; the shaded regions indicate the variance of χ^2 of individual fits, which is the same for the different n values but differs according to line strength because of the different number of pixels used in constraining the fit). The red, green and blue lines indicate the results for *observed* column densities of $\log_{10} N_{\rm obs} = 12, 14, 16$ respectively. Note this means the *intrinsic* central column density increases with decreasing radius. As an example, the inset figure shows the profile for R^{-2} law, $N_{\rm obs} = 10^{14}$, $R_0/R_e = 0.5$, with the best fit plotted in green. By eye the partial coverage is virtually impossible to detect.

We consider a grid of models of varying $N_{\rm obs}$ and R_0, where $N_{\rm obs}$ is the observed (fitted) column density, not the intrinsic column density of the partial absorber. This is achieved by increasing, for each model, the intrinsic column density N_0 until the best fit gives the target $N_{\rm obs}$. The procedure ensures each case we consider is a candidate for an observable system, and automatically includes cases where N_0 is considerably larger than is typically seen in Mg II absorbers but R_0 is very small, which should be the most challenging case to disguise.

The results for $n = 1, 2$ (chosen for the reasons given below) are shown in Figure 1 by dashed and solid lines respectively with $\log_{10} N_{\rm obs} = 12, 14, 16$ in red, green and blue. The shaded regions indicate the 1σ variance on the reduced χ^2 for individual fits: note that this depends on the number of pixels used in its construction, and so will depend on $N_{\rm obs}$ (but not significantly on n or R_0, since $N_{\rm obs}$ is held constant as these are varied).

F06 reproduce their geometric results for profiles as soft

as $n = 1$ ($k = 2$) with core radii $R_0 \sim 0.25$. According to our investigations, individual absorbers in this scenario would be observationally indistinguishable from the complete coverage case, with reduced $\chi^2 \sim 1$ for all fits down to $R_0 = 0.01$. As one increases n (making the absorber edges harder), it rapidly becomes easier to distinguish the cases; for example, for $n = 2$ and $R_0 \sim 0.25$, the high resolution spectra simulated here will highlight a problem. Nevertheless, the χ^2 values presented in Figure 1 represent the poorest possible quality of fit given that the model spectra are of exceptionally high quality and only allow for fitting one velocity component.

Given the results described above, it may appear possible to have a situation in which partial absorption is present but has not been detected in the high resolution data. The physical explanation is simply that the shape of the line depends on N only logarithmically, so allowing N to vary as a shallow powerlaw across the beam does not have a very strong effect: nonetheless, according to F06, one obtains statistical variations in the equivalent width distribution according to the size of the background quasar.

However, with such very slow powerlaw decays, there are further problems to be investigated. On the one hand, the F06 statistical result is valid only in a regime where the differing equivalent widths of observed absorbers is generated by the differing radii of intersection through a population of very similar clouds. On the other hand, there is a very large area over which low column densities may be observed on the periphery of such systems. In particular the observed column density distribution of a single system may be numerically calculated to scale as $\mathrm{d}P(W)/\mathrm{d}W \sim W^{-3}$. It seems unlikely that one could contrive a cosmological distribution of absorbers which provide a rescue from such a steep powerlaw to give the observed $\mathrm{d}P(W)/\mathrm{d}W \sim W^{-1}$ overall distribution (e.g. Narayanan et al. 2007; Churchill et al. 1999) whilst preserving the F06 result for $n = 1$.

In conclusion, it may be that soft edges can be invoked to alleviate somewhat the high resolution fitting problems associated with patchy absorption. However, whilst the limit of extremely shallow outer slopes yields very convincing Voigt profiles, one obtains a new set of statistical challenges. For the rest of this letter, we will assume sharper cut-offs which do not suffer from these problems.

3 Mg II ABSORBERS CLOSE TO C III] λ1909 EMISSION IN QUASAR SPECTRA

If, as in F06, Mg II systems are somewhat smaller than quasar continuum beam widths, it follows that they cannot cover the broad emission line region (Section 1), except with a much reduced column density which must be negligible according to the statistical argument at the end of Section 2. Accordingly, one can approximately model the spectrum over a broad emission line as:

$$F(\lambda) = C(\lambda)e^{-\tau_{\mathrm{MgII}}(\lambda)} + L(\lambda) \quad (4)$$

where F is the received flux, C is the continuum emission flux, L is the broad-line emission flux and τ_{MgII} is the optical depth due to an intervening Mg II system. Assuming (4), an absorber with "intrinsic" equivalent width W (as seen over the continuum region only) will be seen with equivalent width W':

$$W' = \frac{W}{1 + L/C} \quad (5)$$

where $L(\lambda)$ and $C(\lambda)$ are assumed to be constant over the absorption feature (compare typical widths of $20\,\mathrm{kms}^{-1}$ and $5000\,\mathrm{kms}^{-1}$ for a Mg II component and quasar broad line emission respectively). This result applies for any absorber size that is smaller than the continuum region. Possible complications are discussed in Sections 3.3 & 3.4, but essentially this simple model is adequate for our investigation. Equation (5) implies that, for small absorbers, the observed number of absorbers above a specified equivalent width threshold may be reduced significantly over broad line emission features because of the 'diluting' effect of the light from the large broad emission line region. It is thus possible to apply a test similar to the geometric intrinsic/extrinsic test of the Lyα forest described in Sargent et al. (1980).

3.1 Observational Sample

The Mg II λλ2796,2803 absorber sample of Wild et al. (2007, Section 2) is used as the basis for the statistical investigation of the observed absorber properties in the vicinity of the C III] λ1909 emission line. It is derived from a S/N-limited search of 32 278 quasar spectra contained in the Sloan Digital Sky Survey (SDSS) Data Release 4 (DR4) (Adelman-McCarthy et al. 2006). The sample includes absorbers down to a restframe equivalent width (W) of 0.5 Å over an extended redshift range. For our purposes we confine attention to the 2 831 absorbers with $W_0^{2796} \geqslant 0.9$ Å and $-180 < \delta\lambda/\text{Å} < 180$ where $\delta\lambda$ is the wavelength shift between the emission line and absorption line in the quasar restframe:

$$\delta\lambda = \frac{2796\text{Å}(1 + z_{\mathrm{MgII}})}{(1 + z_{\mathrm{quasar}})} - 1909\text{Å} \ . \quad (6)$$

Here z_{MgII} is the redshift of the absorber and z_{quasar} is the redshift of the quasar. The ±180 Å wavelength interval was chosen to provide sufficient absorption lines in the comparison sample. The $W_0^{2796} \geqslant 0.9$ Å limit was chosen to provide an absorber sample consisting of a large number of strong Mg II absorbers but our conclusions are insensitive both to the precise W_0-limit employed or the wavelength extent used to define the comparison sample.

For the test below, we need to predict the absorbers as a function of $\delta\lambda$, without the correction described by equation (5) which will be considered separately. The expected number will be a function of (a) the accessible redshift path, (b) the mean redshift of the absorbers and (c) the S/N in the quasar spectra. The accessible redshift path as a function of $\delta\lambda$ is readily calculated using the redshifts of the base sample of 32 278 quasars. The small systematic change in the number of absorbers due to evolution with redshift can be calculated from the mean absorber redshift as a function of $\delta\lambda$, combined with the absorber number density as a function of redshift, $\propto (1 + z_{\mathrm{MgII}})^{0.23}$, determined by Nestor et al. (2005). The probability of detecting an absorption line of fixed equivalent width varies as a function of S/N. The 'signal' depends on the systematic change in the height of the quasar continuum+C III] λ1909 emission line with $\delta\lambda$. The

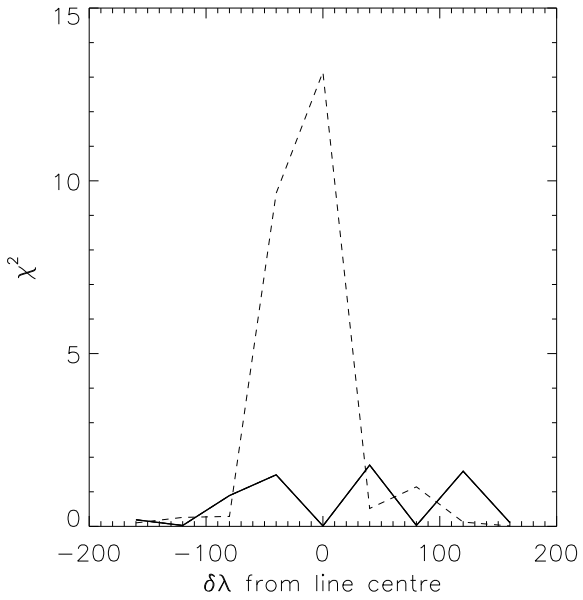

Figure 2. The results of testing for a significant difference between the observed number of absorbers relative to the location of the C III] λ1909 emission line. The thick solid line shows χ^2 for the pure data. The dotted solid line shows χ^2 once the observations are corrected for the partial coverage effect (equation 5); this results in more absorbers entering our sample, changing χ^2. The original data is consistent with predictions, unlike the corrected data, so that we conclude the correction is fictitious.

'noise' varies due to a combination of the increasing sky-background as a function of observed-frame wavelength and of the sensitivity of the SDSS spectrograph and detector. By combining these considerations we can predict the number density of absorbers as a function of $\delta\lambda$.

3.2 Statistical Test

We adopt a very simple statistical test, comparing the predicted number of absorbers with $W_0^{2796} \geqslant 0.9\,\text{Å}$ against the observed number, yielding a value of $\chi^2 = (N_{\rm bin} - N_{\rm exp}(\delta\lambda))^2/N_{\rm exp}(\delta\lambda)$ in bins of 40 Å, where $N_{\rm bin}$ is the observed number of absorbers in the bin and $N_{\rm exp}(\delta\lambda)$ is the expected number of absorbers in the bin according to the procedure detailed above. The bin size is chosen to maximize the number of absorbers per bin whilst ensuring the effect of the broad emission line is not diluted by choosing the bin width too large. The central bin is centred on $\delta\lambda = 0$.

Since one expects, in the absence of partial coverage, $N_{\rm bin}$ to be Poisson distributed with mean $N_{\rm exp}$, and $N_{\rm bin} \sim 300 \gg 1$, the distribution should be accurately Gaussian and χ^2 should be ~ 1 in all bins. However, in the small absorber scenario, the dilution effect will cause a drop in the number of observed absorbers in the vicinity of the broad emission line, and hence an increase in χ^2.

The result is shown by the thick, solid line in Figure 2. The mean $\chi^2 \simeq 0.7$ indicates a result consistent with the full coverage picture. To investigate whether this could occur simply because the effects we look for are too small, we now perform a second test, in which we make the assumption that the observed equivalent widths are altered over the C III] emission line due to partial coverage. In this picture, we have observationally measured W', so each absorber is then adjusted according to (5) to yield W. C is determined by interpolating continuum points from each side of the C III] feature, whilst $L+C$ and hence L may be estimated by inspecting the signal to either side of the Mg II feature. This results in a number of absorbers, which previously had equivalent widths below the 0.9 Å limit, entering our sample. The correction factor to equivalent widths of absorbers on top of the emission feature peaks at $1 + L/C \simeq 1.5$, although there are a few outliers where this factor takes a value as high as $1 + L/C \simeq 2.1$.

Performing the statistical test yields an exceptionally poor fit between the observations and the model predictions, shown by the dashed line in Figure 2. We conclude that the partial coverage scenario is inconsistent with the observations at a very high level of significance, certainly in the simple limit considered here. We now show that the comparison χ^2 results are, in fact, not invalidated by our oversimplification of the absorber model.

3.3 Complication A: Off-Centre Single Absorber

Suppose the continuum region has area A_c, the absorber $A_a \leqslant A_c$ and the broad emission line region has area A_l. If the area overlap between the absorber and continuum is A_0, with total absorber area A_a, it is simple to show that the observed equivalent width W' is given in terms of the intrinsic equivalent width W by:

$$W' = \frac{A_0 A_l C + (A_a - A_0)A_c L}{A_c A_l (C + L)} W \ . \tag{7}$$

Since one could never observe the intrinsic W in this picture, the correct quantity to consider is $W'(L, A_0)/W'(L = 0, A_0)$, i.e. the ratio between the equivalent width observed over an emission line to that observed where there is no emission from the line region:

$$\frac{W'(L, A_0)}{W'(L = 0, A_0)} = \frac{A_0 A_l C + (A_a - A_0)A_c L}{(C + L)A_0 A_l} \ . \tag{8}$$

For $A_0 = A_a$, so that $W'(L = 0, A_0) = W$, this equation correctly reduces to equation (5). However its behaviour elsewhere is somewhat subtle; in the limit $A_0 \to 0$, one obtains $W'(L, A_0)/W'(L = 0, A_0) \to \infty$, apparently compensating for our original effect and generating extra high W absorbers. However, inserting the advocated $A_c \gtrsim 4A_a$, and the observational values $A_l \gtrsim 10A_c$, $L \sim 0.2C$, one can use (7) to show that the population of absorbers generating this compensating effect must have intrinsic $W \gtrsim 250W'$. Thus those absorbers ever to enter our sample ($W' > 0.5$Å) would have physically absurd high intrinsic column densities. We conclude the effects are only significant for $W' \ll 0.5$ Å, so that our statistical result (Section 3.2) is insensitive to these considerations.

3.4 Complication B: Multiple Absorbers

It is clear from the multi-component nature of observed Mg II systems that any single cloud approach is oversimplified. If one asserts the *overall* size of the multi-cloud complex is smaller than the continuum region, our result

holds identically since we have simply shown that there is no detectable net difference in the fraction of light absorbed against the continuum and C III] line regions.

A separate scenario is multiple clouds per sightline, *each* with $A_a \sim A_c$. This would introduce absorption over the broad emission line, thus reducing the magnitude of our comparison χ^2. In Porciani et al. (2007), it is stated that the number of clouds will scale with the beam area. This may or may not be a good approximation to the true behaviour; however, in our opinion the effect cannot be addressed in detail without a sophisticated model which includes considerations of not only the abundance but necessarily the spatial correlation of Mg II systems.

For instance, in a model where Mg II systems cluster in spheres of a characteristic radius, the total number of absorbers over the line region will scale as r^2/A_c where r is the radius of the cluster of absorbers, for $A_L > \pi r^2 > A_c$, but as A_L/A_c for $\pi r^2 > A_L$. This latter scaling is also applicable in the case that Mg II systems are considered to be evenly scattered across the local patch of sky.

Discussion of these models are beyond the scope of this letter. But such considerations do not affect our conclusions with regard to the small Mg II cloud models. The models of F06 are calculated considering only isolated clouds, and already these clouds must be adjusted in size to fit the data. In order to simultaneously fit our negative result and the GRB/quasar mismatch, one would need additionally to model the distribution of clouds so that the approximation breaks down in the correct manner and at the correct scale to compensate precisely for the geometric dilution in our specific case. Such a degree of fine tuning would not be acceptable without the support of a physically motivated model.

4 CONCLUSIONS

We investigated the possibility that Mg II absorber clouds are somewhat smaller than, but comparable to, the beam width of the quasar continuum. Such a scenario is motivated by disparate statistics of Mg II absorption when comparing GRB and quasar sightlines (F06).

All our results suggest that, without extreme fine-tuning, the model is hard to match with the known properties of Mg II systems. High resolution spectroscopy directly rules out partial coverage clouds with hard edges, whilst softening the edge will mimic a pure Voigt profile well but introduce difficulties with producing the known equivalent width distribution. Most convincingly, a statistical test for systematically lowered equivalent widths over quasar broad line emission regions (which are substantially larger than quasar continuum regions) produces no result. After applying a correction on the assumption that partial coverage is the correct scenario, an inconsistency between the equivalent width distributions over broad emission line and continuum regions arises. The only circumstances in which the F06 model holds and our broad emission line effect might be unobservable are those in which extreme fine tuning of the sizes and distributions are invoked (Section 3.4).

We therefore reject the proposition of Mg II absorbers which are patchy on scales comparable to quasar continuum beam sizes. The true explanation for the observations of Prochter et al. (2006) remains elusive.

ACKNOWLEDGMENTS

We thank Max Pettini and Berkeley Zych for useful comments on a draft of this letter. AP is supported by a STFC (formerly PPARC) studentship and scholarship at St John's College, Cambridge. VW is supported by the MAGPOP Marie Curie EU Research and Training Network.

REFERENCES

Adelman-McCarthy, J. K., et al. 2006, ApJS, 162, 38
Bouché, N., Murphy, M. T., & Péroux, C. 2004, MNRAS, 354, L25
Churchill, C. W. 1997, PhD thesis, AA (University of California, Santa Cruz)
Churchill, C. W., Rigby, J. R., Charlton, J. C., & Vogt, S. S. 1999, ApJS, 120, 51
Frank, S., Bentz, M. C., Stanek, K. Z., Dietrich, M., Kochanek, C. S., Mathur, S., & Peterson, B. M. 2006, preprint (astro-ph/0605676)
Narayanan, A., Misawa, T., Charlton, J. C., & Kim, T.-S. 2007, ApJ, 660, 1093
Hao, H., Stanek, K. Z., Dobrzycki, A., Matheson, T., Bentz, M. C., Kuraszkiewicz, J., Garnavich, P. M., Howk, J. C., Calkins, M. L., Worthey, G., Modjaz, M., & Serven, J. 2007, ApJ, 659, L99
Kaspi, S., Maoz, D., Netzer, H., Peterson, B. M., Vestergaard, M., & Jannuzi, B. T. 2005, ApJ, 629, 61
Kaspi, S., Brandt, W. N., Maoz, D., Netzer, H., Schneider, D. P., & Shemmer, O. 2007, ApJ, 659, 997
Lewis, G. F., Irwin, M. J., Hewett, P. C., & Foltz, C. B. 1998, MNRAS, 295, 573
Nestor, D. B., Turnshek, D. A., & Rao, S. M. 2005, ApJ, 628, 637
Porciani, C., Viel, M., & Lilly, S. J. 2007, ApJ, 659, 218
Prochter, G. E., Prochaska, J. X., Chen, H.-W., Bloom, J. S., Dessauges-Zavadsky, M., Foley, R. J., Lopez, S., Pettini, M., Dupree, A. K., & Guhathakurta, P. 2006, ApJ, 648, L93
Rauch, M., Sargent, W. L. W., Barlow, T. A., & Simcoe, R. A. 2002, ApJ, 576, 45
Sargent, W. L. W., Young, P. J., Boksenberg, A., & Tytler, D. 1980, ApJS, 42, 41
Steidel, C. C. 1993, in Astrophysics and Space Science Library, Vol. 188, Astrophysics and Space Science Library, ed. J. M. Shull & H. A. Thronson, 263–+
Sudilovsky, V., Savaglio, S., Vreeswijk, P., Ledoux, C., Smette, A., & Greiner, J. 2007, preprint (arXiv:0705.0706)
Tejos, N., Lopez, S., Prochaska, J. X., Chen, H.-W., & Dessauges-Zavadsky, M. 2007, preprint (arXiv:0705.0387)
Wayth, R. B., O'Dowd, M., & Webster, R. L. 2005, MNRAS, 359, 561
Wild, V., Hewett, P. C., & Pettini, M. 2007, MNRAS, 374, 292
Zibetti, S., Ménard, B., Nestor, D. B., Quider, A. M., Rao, S. M., & Turnshek, D. A. 2007, ApJ, 658, 161